SAN FRANCISCO ESTUARY & WATERSHED SCIENCE
Sponsored by the Delta Science Program and UC Davis Institute for the Environment

RESEARCH

Investigating Factors that Contribute to Phytoplankton Biomass Declines in the Lower Sacramento River

Timothy D. Mussen*[1], Sara Driscoll[2], Michael E. Cook[3], Justin D. Nordin[3], Marianne Guerin[4], Richard Rachiele[4], Donald J. Smith[4], Gry Mine Berg[5], Lisa C. Thompson[1]

ABSTRACT

Phytoplankton subsidies from river inputs and wetland habitats can be important food sources for pelagic organisms in the Sacramento–San Joaquin Delta (Delta). However, while the Sacramento River is a key contributor of water to the Delta, providing 80% of the mean annual inflow, the river is only a minor source of phytoplankton to the system. The reason for low phytoplankton biomass in the Sacramento River is not well understood but appears to be associated with a 65-km stretch of the lower river where chlorophyll-*a* (Chl-*a*) concentrations can decline by as much as 90%. We conducted two surveys along the lower Sacramento River, in spring and fall of 2016, to investigate the relative contributions of different factors potentially driving this Chl-*a* decline. Our study evaluated the change in Chl-*a* concentrations as a result of dilution from tributaries, light availability, nutrient concentrations, nutrient uptake, phytoplankton productivity, zooplankton grazing, and clam grazing. Chl-*a* concentration decreased from 14 $\mu g\,L^{-1}$ to 1.8 $\mu g\,L^{-1}$ in the spring and from 4.0 $\mu g\,L^{-1}$ to 1.2 $\mu g\,L^{-1}$ in the fall. Dilutions from the Feather River and American River contributed 39% and 11% of Chl-*a* declines, respectively, during the spring. Average water depths roughly doubled downstream of the American River confluence, reducing water column light availability and lowering productivity. Zooplankton and clam grazing rates were generally low. Using a mass balance analysis, the measured variables explained 76% of the observed decline in Chl-*a* in the spring, suggesting additional losses from unidentified factors. We found that phytoplankton biomass is regulated by multiple potential factors in the lower Sacramento River, emphasizing the need for practitioners of restoration and management programs to evaluate multiple potential factors when attempting to enhance phytoplankton production in the Delta, or other large river systems.

SFEWS Volume 21 | Issue 1 | Article 3

https://doi.org/10.15447/sfews.2023v21iss1art3

* Corresponding author: *mussent@sacsewer.com*

1 Sacramento Area Sewer District and Sacramento Regional County Sanitation District Sacramento, CA 95827 USA

2 Alfred–Wegener Institute Helmholtz Centre for Polar and Marine Research D-27570 Bremerhaven, Germany

3 Sacramento Regional Wastewater Treatment Plant Elk Grove, CA 95758

4 Resource Management Associates, Inc. Davis, CA 95618 USA

5 Environmental Science Associates Sacramento, CA 95816 USA

KEY WORDS

Phytoplankton, productivity, euphotic zone, dilution, residence time, nutrients, nitrogen uptake, clam, zooplankton, grazing

INTRODUCTION

The Sacramento River is the largest river in California and travels 644 km from Mount Shasta to the San Francisco Estuary (estuary). This key waterway drains an area of approximately 70,000 km^2 and contributes an important fraction of the freshwater supply and nutrients that support the food webs of the Sacramento–San Joaquin Delta (the Delta) and estuary (Domagalski et al. 2000; Kimmerer 2004; Jassby 2008; Novick and Senn 2014; Beck et al. 2018). Primary productivity in the Sacramento River and throughout the estuary is low compared with other river-dominated estuaries (Boynton et al. 1982; Jassby et al. 2002; Cloern et al. 2014). Pelagic communities in the Delta rely on subsidies of phytoplankton and zooplankton from upstream tributaries and tidal wetlands (Lehman et al. 2010; Kimmerer and Thompson 2014; Brown et al. 2016; Kimmerer et al. 2019), although not all Delta wetlands provide positive fluxes of zooplankton into the larger channels (Lehman et al. 2010; Kimmerer et al. 2018). While the Sacramento River provides 80% of the mean daily inflow to the Delta (CDWR 2020), the river is only a minor source of phytoplankton and net primary productivity to the Delta system (Jassby et al. 2002). Between 1989 and 2019, phytoplankton biomass in the lower Sacramento River, as indicated by Chl-*a* concentration at river mile (RM) 38, averaged 2.1 $\mu g\,L^{-1}$ (IEP 2020). In the Delta, Chl-*a* concentration below 10 $\mu g\,L^{-1}$ can limit the rate of zooplankton growth (Müller–Solger et al. 2002). Dodds and Smith (2016) have also suggested that suspended Chl-*a* less than 10 $\mu g\,L^{-1}$ is a trophic boundary for oligotrophic conditions in rivers and streams. A several-fold decrease in Chl-*a* between the upstream and downstream regions of the lower Sacramento River has been reported in several investigations. For example, Parker et al. (2012) documented a decline in Chl-*a* from 9 $\mu g\,L^{-1}$ to 2 $\mu g\,L^{-1}$ between RM 60 and RM 27 in April of 2009, and Glibert et al. (2014) reported a decline from 20 $\mu g\,L^{-1}$ to 1.6 $\mu g\,L^{-1}$ between RM 63 and RM 19 in March of 2014. Along the same stretch of the Sacramento River, Kraus et al. (2017) reported a decline in Chl-*a* from 15 $\mu g\,L^{-1}$ to 2.5 $\mu g\,L^{-1}$ in October of 2013 and a decline from 25 $\mu g\,L^{-1}$ to 2.5 $\mu g\,L^{-1}$ in June of 2014.

The conditions leading to this decline in Chl-*a* have been the subject of many recent investigations. For example, light limitation is a widely recognized factor for regulating intrinsic phytoplankton growth in the estuary and in the Delta (Cole and Cloern 1984, 1987; Alpine and Cloern 1988) and was recently demonstrated to be an important factor for regulating phytoplankton growth in the Sacramento River (Strong et al. 2021). Another potentially important factor is rapid water velocities leading to short residence times (Jassby 2008; Hammock et al. 2019), which prevents accumulation of phytoplankton biomass in a given area or region. Grazing is another potential regulator of phytoplankton biomass. The invasive freshwater clam (*Corbicula fluminea*) and the brackish water clam (*Potamocorbula amurensis*) can consume large quantities of phytoplankton in the Delta (Lopez et al. 2006; Cloern and Jassby 2012; Kimmerer and Thompson 2014). Patches of high clam biomass have also been noted in the Sacramento River (Kraus et al. 2017). Toxicity from pesticides associated with agricultural, urban, or treated wastewater discharge into the Sacramento River may also negatively affect primary production and phytoplankton biomass accumulation (Orlando et al. 2014; Lam et al. 2019). Similarly, high ammonium concentrations in effluent from the Sacramento Regional Wastewater Treatment Plant (SRWTP) outfall have been hypothesized to negatively affect phytoplankton productivity in the Sacramento River and upper estuary (Dugdale et al. 2007; Parker et al. 2012). However, findings from multiple recent papers reviewed in Cloern (2021) call this hypothesis into question.

Ideally, all the factors that regulate phytoplankton biomass and potentially contribute to phytoplankton declines along the lower Sacramento River should be characterized and

examined simultaneously. In an effort to assess the relative importance of physical (dilution, light), chemical (nutrients and pollutants), and biological (phytoplankton productivity, zooplankton grazing, clam grazing) factors, we conducted two surveys along the lower 160-km portion of the Sacramento River. We then used a simple mass balance analysis to examine the relative importance of the different factors potentially altering Chl-*a* concentrations between sampling stations. Our goals were to investigate how far up the Sacramento River the trend in Chl-*a* decline started, to quantify the relative importance of factors that contribute to Chl-*a* decline along the entire lower portion of the river, and to identify regions of the river where the observed change in Chl-*a* differed from the values predicted by the mass balance analysis.

MATERIALS AND METHODS

Survey Sites

We conducted two surveys along the lower 122-km portion of the Sacramento River and its tributaries in the spring (May 9–13) and fall (October 24–28) of 2016 onboard the R/V *Guardian*. During each survey, 16 locations were sampled from the northernmost station at RM 95 to the southernmost station near the mouth of the Sacramento River at RM 19 (Figure 1). Eleven of our sampling stations were in the mainstem of the Sacramento River, and five were in tributaries that feed into the Sacramento River. All tributaries—including the Colusa Basin Drain, the East Canal, the Feather River, the Natomas Cross Canal, and the American River—were sampled upstream of their confluence with the Sacramento River. At each station, we sampled water temperature, dissolved oxygen (DO) concentration, pH, specific conductance, turbidity, vertical profiles of photosynthetically active radiation (PAR), dissolved inorganic nutrient concentrations, phytoplankton nitrogen and carbon uptake rates, Chl-*a* concentration, phytoplankton species abundances and biovolumes, zooplankton species abundances and biovolumes, and clam abundances and biomass.

Water Source Calculations

We used water flow rates and volumes to calculate fully mixed proportions of water at downstream sampling stations from five modeled water sources using a volumetric hydrological model developed and calibrated by Resource Management Associates (RMA; Guerin 2018). Water sources in the model included: upper Sacramento River inflows into our study region, the Feather River, the East Canal, the American River, and treated wastewater effluent from SRWTP. The model combined Colusa Basin Drain and upper Sacramento River flows in the spring, and no outflow occurred in the Colusa Basin Drain during the fall. No records were available to quantify outflows from the Natomas Cross Canal. We used cross-river, high-frequency, electrical conductivity measurements in a simple two-component mixing model to validate the proportions of modeled water sources below tributary confluences. We calculated travel times between sampling stations using a particle-tracking model with hourly time-steps.

Water Column Sampling and Analyses

At each station, we deployed a YSI model 6600 sonde (Xylem Instruments) with an integrated LI-COR underwater quantum sensor (model LI-192SA) to collect vertical profiles of PAR (µmol photons m^{-2} s^{-1}), temperature (°C), pH, electrical conductivity (µS cm^{-1}), DO (mg L^{-1}) and depth (m). The sonde was housed in a steel cage and had a lead weight attached to the bottom to ensure it remained vertical during profiling. We collected surface water (~0.5 m depth) samples mid-day and mid-channel using a peristaltic pump and an acid-cleaned plastic bucket. We filtered samples for analyses of dissolved inorganic nutrient concentrations through a 0.45-µm filter, preserved, and stored refrigerated until analysis at the Regional San Environmental Laboratory. We analyzed ammonium (NH_4^+), nitrate plus nitrite ($NO_3^- + NO_2^-$), total dissolved phosphate (PO_4^{3-}), dissolved silica, and dissolved inorganic carbon (DIC) using EPA methods 350.1, 353.2, 365.4, 200.8, and standard method 5310B, respectively. At each site, turbidity was measured using a Hach 2100P turbidimeter (EPA method 180.1). For Chl-*a* determination, we

https://doi.org/10.15447/sfews.2023v21iss1art3

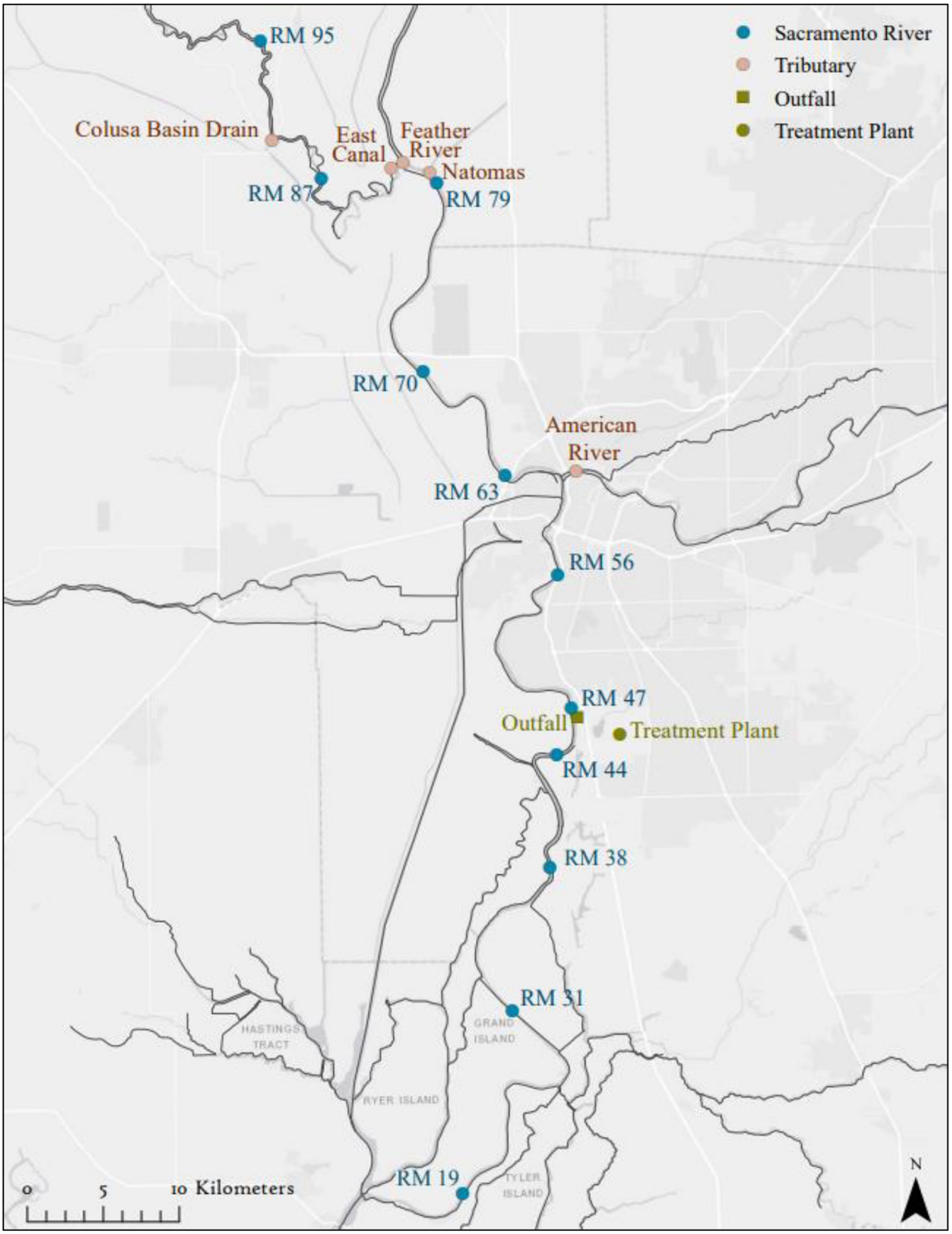

Figure 1 Locations of stations sampled along the Sacramento River. Mainstem stations in *blue*, stations sampled in tributaries in *red*, and the Sacramento Regional Wastewater Treatment Plant and its wastewater outfall location in *green*.

analyzed collected samples following standard method 10200 H. Briefly, 20 ml to 100 ml volume was filtered onto Whatman GF/F filters, which were placed in petri dishes, wrapped in foil, and preserved frozen until analysis. Frozen samples were ground using a Teflon-coated tissue grinder (Wheaton) with 90% acetone for 1 to 2 min. The ground filter was rinsed with 90% acetone into a centrifuge tube to extract overnight in a dark refrigerator. We then centrifuged samples and analyzed the supernatant at 750 nm using a spectrophotometer.

We collected whole water samples for phytoplankton, picoplankton, and zooplankton enumerations and shipped them to BSA Environmental, Inc. for analysis. Briefly, whole water samples were collected in brown HDPE bottles and preserved with Lugol's solution (5 ml per 250 ml water sample). Preserved samples were filtered onto 0.2-µm polycarbonate membranes (Nuclepore) and enumerated using a Leica DMLB compound microscope, according to McNabb (1960) as described in Beaver et al. (2013). At least 400 natural units (colonies, filaments, and unicells) were enumerated to the lowest possible taxonomic level from each sample. The abundances of common taxa were estimated by random field counts. Rare taxa were quantified by scanning a transect of the filter. In the case of rare, large taxa, half of the filter was scanned and counted at a lower magnification. Cell volumes (biovolumes) were estimated by applying the geometric shapes that most closely matched the cell shape (Hillebrand et al. 1999). Biovolume calculations were based on measurements of 10 organisms per taxon in each sample, when possible. The contribution of small (<2-µm-diameter) chlorophyll-containing phytoplankton cells, hereafter called "picoplankton", to total phytoplankton community biovolume was estimated separately. Briefly, 50-ml whole water samples were preserved with 50% gluteraldehyde and stored refrigerated. Picoplankton samples were filtered onto 0.2-µm polycarbonate membranes (Nuclepore), enumerated, and sized using an epifluorescence microscope.

Nitrogen and Carbon Uptake

Rates of nitrogen uptake were measured by addition of ^{15}N-labeled nitrate ($^{15}N\text{-}NO_3^-$) and ammonium ($^{15}N\text{-}NH_4^+$), and rates of carbon uptake by addition of ^{13}C-labeled bicarbonate. Whole water samples were collected using an acid-cleaned plastic bucket, which was rinsed three times with ambient river water before filling. Water was transferred into acid-cleaned 250-ml polycarbonate square bottles (Nalgene) after rising each bottle three times. Trace concentrations (approximately 10% of ambient nutrient concentration) of $^{15}N\text{-}NO_3^-$, varying from 0.05 to 0.8 µmol L^{-1} depending on location in river, were added to triplicate bottles. Similarly, trace concentrations of $^{15}N\text{-}NH_4$+, ranging from 0.05 to 4 µmol L^{-1}, were added to another set of triplicate bottles giving a total of six bottles for each station. ^{13}C-bicarbonate was added to all six incubation bottles at a final concentration of 100 µmol L^{-1}. Bottles spiked with labels were placed into a flow-through incubator on deck and shaded with two layers of darkened, neutral-density netting (top and sides) that transmitted 40% of surface irradiance. Uptake incubations were terminated after 4 h by vacuum filtering 125 to 250 mL onto combusted 25-mm Whatman glass fiber filters. Filters were placed in sterile 2-mL Eppendorf microcentrifuge tubes and dried at 50 °C overnight in a drying oven. After drying, samples were stored in a desiccator until they were processed for mass spectrometric analysis at the Stable Isotope Facility, University of California, Davis. Specific uptake rates (V) of nitrogen and carbon (hereafter uptake rates) were calculated according to Glibert and Capone (1993),

$$V(h^{-1}) = \frac{Atom\%excess}{Atom\%enrichment \times time} \quad (1)$$

where atom % excess is the enrichment of the particulate matter collected on the filter above atmospheric background concentrations and atom % enrichment is the enrichment of the dissolved pool. Carbon uptake rates (h^{-1}) were multiplied by the number of daylight hours to obtain the maximum (also referred to as intrinsic gross) phytoplankton growth rates (μ_{max}, d^{-1}) used in our Chl-*a* mass balance calculation. We compared

https://doi.org/10.15447/sfews.2023v21iss1art3

the mean nitrogen and carbon uptake rates separately, between the four sample locations immediately upstream of the SRWTP outfall (which is located at RM 46.3) and the four sample locations immediately downstream of the SRWTP outfall, using two-tailed *t* tests (alpha = 0.05) to determine if uptake rates were affected by the presence of treated wastewater effluent during the spring or fall surveys.

Macrozooplankton Sampling

We sampled macrozooplankton at each station by vertical net tows, using 12-cm-diameter nets with 153-µm mesh. We also sampled microzooplankton by vertical net tows, using 12-cm-diameter nets with 35-µm mesh, but microzooplankton biomass was negligible compared with the macrozooplankton and was therefore not included in our mass balance calculations. Three macrozooplankton samples were collected at each station, using one to six vertical tows per sample, ranging from 2 to 10 m in length, depending on water depth and the density of material in the water column. After rinsing the net three times, samples were transferred from the cod end to 250-mL brown HDPE bottles and preserved with Lugol's solution (12.5 ml per 250 ml water sample). Preserved macrozooplankton samples were analyzed by BSA using the Utermohl technique with a minimum tally of 200 organisms. Dry weight biomass was estimated based on length and length-to-width relationships (Beaver et al. 2010).

Clam Collections and Analysis

We collected adult (> 5 mm) *C. fluminea* clams from the riverbed with a 35-cm-wide trawling dredge. At each station, five transects were dredged parallel to the river banks, with transects spaced equally across the river's width. On average, the trawl was towed for 1 min at 1.8 km h^{-1}. Collected clams were placed in mesh bags and held in chilled coolers for < 10 h during transport to the laboratory, where they were fixed in 10% formalin for 7 days, and then preserved in 70% ethanol. We measured clam shell widths with calipers and calculated ash-free dry weight (AFDW, g) for each individual clam using an empirical conversion formula. Clam biomass per m^2 was calculated by dividing the total clam biomass by the area sampled for each river transect. We estimated clam grazing rates per station from the mean clam biomass according to Lopez et al. (2006) and assumed a grazing efficiency of 100%.

Chl-a Mass Balance Calculation

A mass balance calculation (e.g., Caraco et al. 1997) was used to estimate changes in Chl-*a* concentrations between each of our sampling stations based on measured biomass and measured rate variables at each station. The analysis was started at the uppermost station (RM 95) in the Sacramento River, using the measured Chl-*a* concentration of 14 µg Chl-*a* L^{-1} in spring and 2.7 µg Chl-*a* L^{-1} in fall. The estimated Chl-*a* concentration for each sequential station (Chl_b) was calculated by adding changes in Chl-*a*—resulting from phytoplankton growth, variation in light availability, phytoplankton respiration, grazing by clams, grazing by zooplankton, and dilution by additions of water from tributaries—to the upstream Chl-*a* concentration (Chl_{b-1}). We assumed no changes in river flows from groundwater input or atmospheric deposition. Travel time (t) between stations was determined by RMA's particle-tracking model (Guerin 2018). The mass balance equation is shown below:

$$Chl_b(\mu g\ L^{-1}) = \left[Chl_{b-1} + Chl_{b-1}(\mu - r - G_{zp} - CT)t\right]D + Chl_t(1 - D) \quad (2)$$

where µ (d^{-1}) is phytoplankton growth rate, *r* (d^{-1}) is basal plus variable respiration, G_{zp} (d^{-1}) is zooplankton grazing rate, *CT* (d^{-1}) is clam turnover rate, *D* is a unitless dilution factor that reflects the ratio of upstream Sacramento River flow to the total flow (including any tributary flow that enters at the location), and Chl_t is the Chl-*a* concentration in the joining tributary. We compared calculated Chl-*a* concentrations from the mass balance analysis to measured Chl-*a* concentrations at each sampling station on the Sacramento River to gauge how well the factors we tested explained the observed Chl-*a* declines in the river. See Appendix A for further details including equations used for the different terms in the Chl-*a* mass balance analysis.

RESULTS

Water Source Calculations

In spring, the Sacramento, Feather, and American rivers had similar flow rates (Figure 2A). In fall, the Feather River contributed close to 40%, while the American River contributed 10% of the water volume in the lower Sacramento River mainstem downstream of their confluences (Figure 2B). The East Canal contributed between 5% to 8% of the total Sacramento River volume during both seasons, and the water volume from SRWTP effluent discharge was negligible. Sacramento River discharge in both spring (i.e., May) and fall (i.e., October) was moderate compared to flows present in March and April 2016 (Appendix B, Figure B1). Tidally-averaged water velocities in the river transect varied between 15 km d^{-1} to 56 km d^{-1} in spring and between 13 km d^{-1} to 42 km d^{-1} in fall, with the fastest velocities occurring in the middle segments of the river and the lowest velocities occurring around Isleton at RM 19 (Table 1).

Water Column Sampling and Analyses

Water in the Sacramento River and its tributaries was well mixed in both spring and fall, according to vertical profiles of water temperature, conductivity, and salinity. As a result, the total water column depth was identical to the mixing depth (Z_m). Mean water temperature throughout the study region was 20 ± 1.0 °C (mean ± SE) in spring and 16 ± 1 °C in the fall, with the exception of 13.5 °C water in the American River during the spring (Table 1). Compared to the Sacramento River mainstem, the Colusa Basin Drain and East Canal had greater conductivities, and the American River had lower conductivity, in both seasons. DO concentrations were lower in the East Canal and Natomas Cross Canal compared to Sacramento River mainstem stations in both seasons, and the Colusa Basin Drain had elevated DO in the fall (Table 1). Turbidities were higher in spring than fall and decreased from the upper to the lower reaches of the Sacramento River. During spring, turbidity in the Sacramento River was stable before and during our week of sampling (Appendix B, Figure B1). The diffuse attenuation

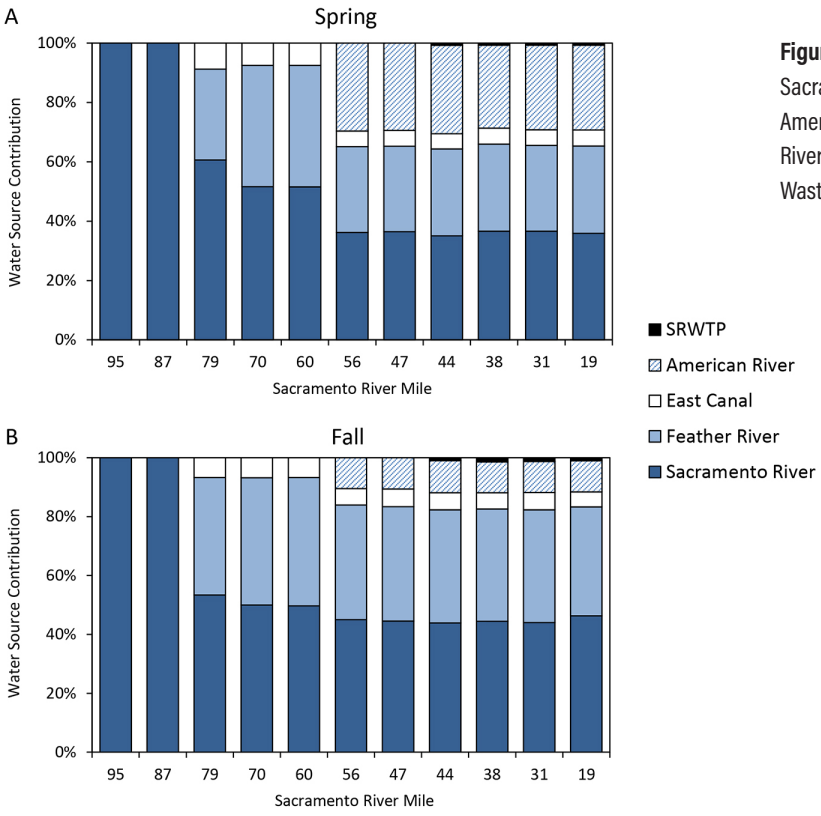

Figure 2 Contributions to water volume in the lower Sacramento River (between RM 95 and RM 19) from the American River, East Canal, Feather River, upstream Sacramento River, and wastewater effluent from the Sacramento Regional Wastewater Treatment Plant, in (**A**) spring and (**B**) fall.

https://doi.org/10.15447/sfews.2023v21iss1art3

Table 1 Station names, locations, depths, and water-column characteristics in spring and fall. Sacramento River Mile zero set at the confluence with the San Joaquin River, near Collinsville, CA. Sacramento River mainstem water velocities and travel times between mainstem stations were derived from the Resource Management Associates particle-tracking model and are not available for tributaries (Guerin 2018).

Station	Name	Location	River Mile	Latitude	Longitude	Depth (m)	Temp. (°C)	Conduc. (µS cm^{-1})	pH	DO (mg L^{-1})	Turbidity (NTU)	Kd (m^{-1})	Velocity (km d^{-1})	Travel time (d^{-1})
Spring														
1	Upper River	Mainstem	95	38.51.582	121.43.866	3.5	18.9	166	8.6	9.5	49.4	1.8	21	—
2	Colusa Basin Drain	Tributary	90	38.48.068	121.43.402	2.0	19.8	449	8.2	8.5	95.5	4.9	—	—
3	Knights Landing	Mainstem	87	38.46.709	121.41.188	4.8	18.9	224	8.0	9.0	30.5	2.0	21	0.38
4	East Canal	Tributary	81	38.47.015	121.37.986	5.1	20.7	372	7.6	6.0	32.3	2.5	—	—
5	Feather River	Tributary	80	38.47.214	121.37.449	1.9	18.3	84	8.4	9.5	23.9	1.3	—	—
6	Natomas Cross Canal	Tributary	79	38.46.818	121.36.248	2.1	20.9	148	8.3	7.8	24.7	2.4	—	—
7	Verona	Mainstem	79	38.46.480	121.35.957	2.7	19.7	157	8.1	9.1	17.5	1.9	27	0.29
8	I5 Bridge	Mainstem	70	38.39.779	121.36.699	2.3	20.3	171	8.4	8.9	30.4	1.8	27	0.33
9	I80 Bridge	Mainstem	63	38.36.042	121.33.069	3.2	20.0	166	8.2	8.8	22.0	1.9	28	0.25
10	American River	Tributary	60	38.36.150	121.29.845	2.6	13.5	59	8.5	9.9	3.4	0.6	—	—
11	Land Park	Mainstem	56	38.32.493	121.30.742	9.0	18.1	136	8.2	9.0	10.1	1.1	56	0.13
12	Freeport	Mainstem	47	38.27.736	121.30.227	7.0	19.3	131	8.2	9.0	8.5	1.0	24	0.38
13	RM44	Mainstem	44	38.26.090	121.30.926	8.9	19.0	146	8.0	9.0	7.5	1.0	24	0.13
14	Hood	Mainstem	38	38.22.114	121.31.329	7.8	18.5	148	7.7	8.8	8.0	1.0	20	0.25
15	Steamboat Slough	Mainstem	31	38.17.036	121.33.125	9.2	19.4	144	7.4	8.9	6.1	0.8	24	0.33
16	Isleton	Mainstem	19	38.10.588	121.35.467	4.6	21.1	145	7.9	8.7	5.8	1.0	15	0.79
Fall														
1	Upper River	Mainstem	95	38.51.582	121.43.866	3.1	15.2	150	7.7	9.8	6.0	2.5	21	—
2	Colusa Basin Drain	Tributary	90	38.48.068	121.43.402	1.4	16.4	461	8.0	10.1	13.3	2.8	—	—
3	Knights Landing	Mainstem	87	38.46.709	121.41.188	3.4	15.2	145	8.0	9.9	8.2	1.2	21	0.38
4	East Canal	Tributary	81	38.47.015	121.37.986	3.7	16.9	396	7.5	7.1	16.3	0.9	—	—
5	Feather River	Tributary	80	38.47.214	121.37.449	2.0	15.5	127	7.6	9.6	4.2	3.1	—	—
6	Natomas Cross Canal	Tributary	79	38.46.818	121.36.248	1.6	16.5	154	8.1	6.9	4.8	0.7	—	—
7	Verona	Mainstem	79	38.46.480	121.35.957	2.2	15.7	147	8.1	9.6	7.2	3.7	24	0.33
8	I5 Bridge	Mainstem	70	38.39.779	121.36.699	2.4	16.0	146	7.9	9.3	7.0	2	24	0.38
9	I80 Bridge	Mainstem	63	38.36.042	121.33.069	2.6	16.0	145	8.0	9.0	5.1	1.6	24	0.29
10	American River	Tributary	60	38.36.150	121.29.845	5.0	17.0	60	7.6	9.1	2.0	0.8	—	—
11	Land Park	Mainstem	56	38.32.493	121.30.742	6.7	15.9	135	7.8	9.3	5.3	1.3	42	0.17
12	Freeport	Mainstem	47	38.27.736	121.30.227	7.3	16.2	74	7.6	9.1	3.4	2.5	14	0.67
13	RM44	Mainstem	44	38.26.090	121.30.926	6.8	16.4	76	7.5	9.4	3.4	2.8	24	0.13
14	Hood	Mainstem	38	38.22.114	121.31.329	6.7	16.3	78	7.6	9.2	4.0	2.7	15	0.33
15	Steamboat Slough	Mainstem	31	38.17.036	121.33.125	7.4	16.5	166	7.4	8.9	4.8	0.8	15	0.54
16	Isleton	Mainstem	19	38.10.588	121.35.467	3.8	16.5	148	7.5	8.8	5.3	0.7	13	0.92

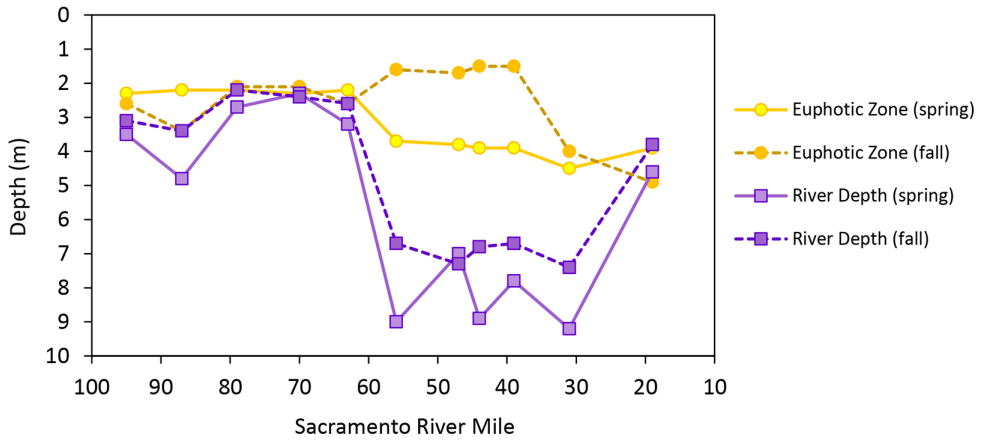

Figure 3 Euphotic depths (yellow circles) and water depths (purple squares) at stations sampled along the Sacramento River in the spring (*solid*) and fall (*dashed*).

coefficient for downwelling PAR (K_d) in the Sacramento River mainstem decreased from upstream to downstream, ranging from 3.7 to 0.7 m^{-1} (Table 1). The depth of the euphotic zone (Z_{eu}) calculated as $4.6/K_d$ was compared to Z_m. The Z_{eu}:Z_m ratio was reduced below RM 63, as a result of increased river depths (Figure 3).

Nutrient Concentrations, Nitrogen Uptake, and Productivity Measurements

In the spring transect, NO_3^- concentrations in the Sacramento River mainstem upstream of SRWTP's outfall (between RM 95 to RM 47) varied from 7.6 µmol L^{-1} to 11.0 µmol L^{-1}, and NH_4^+ concentrations varied from 1.4 µmol L^{-1} to 6.7 µmol L^{-1} (Figure 4A). NO_3^- concentrations below SRWTP's outfall (between RM 44 and RM 19) were similar to those upstream, while NH_4^+ concentrations increased, varying from 23.6 to 46.4 µmol L^{-1} (Figure 4A). Therefore, the average contribution of NH_4^+ to dissolved inorganic nitrogen (including nitrate, nitrite, and ammonium) was 23% upstream of SRWTP's outfall and 76% below. Among the tributaries, the Colusa Basin Drain had the greatest nitrogen concentration in the spring, where NO_3^- was 19.5 µmol L^{-1} and NH_4^+ was 10.0 µmol L^{-1}.

In the fall, nitrogen concentrations in the Sacramento River mainstem were greater than during spring (Figure 4B). Concentrations of NO_3^- above the SRWTP outfall varied from 11.9 µmol L^{-1} to 14.3 µmol L^{-1}, and NH_4^+ from 1.9 µmol L^{-1} to 4.5 µmol L^{-1}. Below the SRWTP outfall, NO_3^- varied from 11.4 µmol L^{-1} to 21.2 µmol L^{-1}, and NH_4^+ from 40.7 µmol L^{-1} to 66.2 µmol L^{-1}. During the fall sampling, there was no outflow from the Colusa Basin Drain to the Sacramento River, and NO_3^- and NH_4^+ concentrations in the Colusa Basin Drain were the lowest observed at any station (Figure 4B). Concentrations of PO_4^{3-} were relatively consistent throughout the length of the Sacramento River mainstem in spring and fall, averaging 2.0 ± 0.2 µmol L^{-1} (mean ± SE), (Figures 4A and B). The average dissolved silica concentration in the Sacramento River was 287 ± 15.7 µmol L^{-1} (mean ± SE) in the spring and 143.0 ± 8.9 µmol L^{-1} in the fall.

Uptake of NH_4^+ contributed the majority of total nitrogen uptake (NH_4^+ uptake + NO_3^- uptake) in the Sacramento River mainstem in the spring transect, both upstream (74%) and downstream (91%), as well as in the tributaries (Figure 4C). In the spring, uptake rates of NH_4^+ averaged 0.012 h^{-1} between RM 95 and RM 47 (Figure 4C). At RM 44, where NH_4^+ concentrations increased sharply, the NH_4^+ uptake rate increased 2.4-fold to 0.03 h^{-1} before decreasing to 0.018 h^{-1} between stations RM 38 and RM 19 (Figure 4C). The average total nitrogen uptake rate (0.013 h^{-1}) for the four stations above SRWTP's outfall (RM 70 to RM 47) was significantly lower compared

https://doi.org/10.15447/sfews.2023v21iss1art3

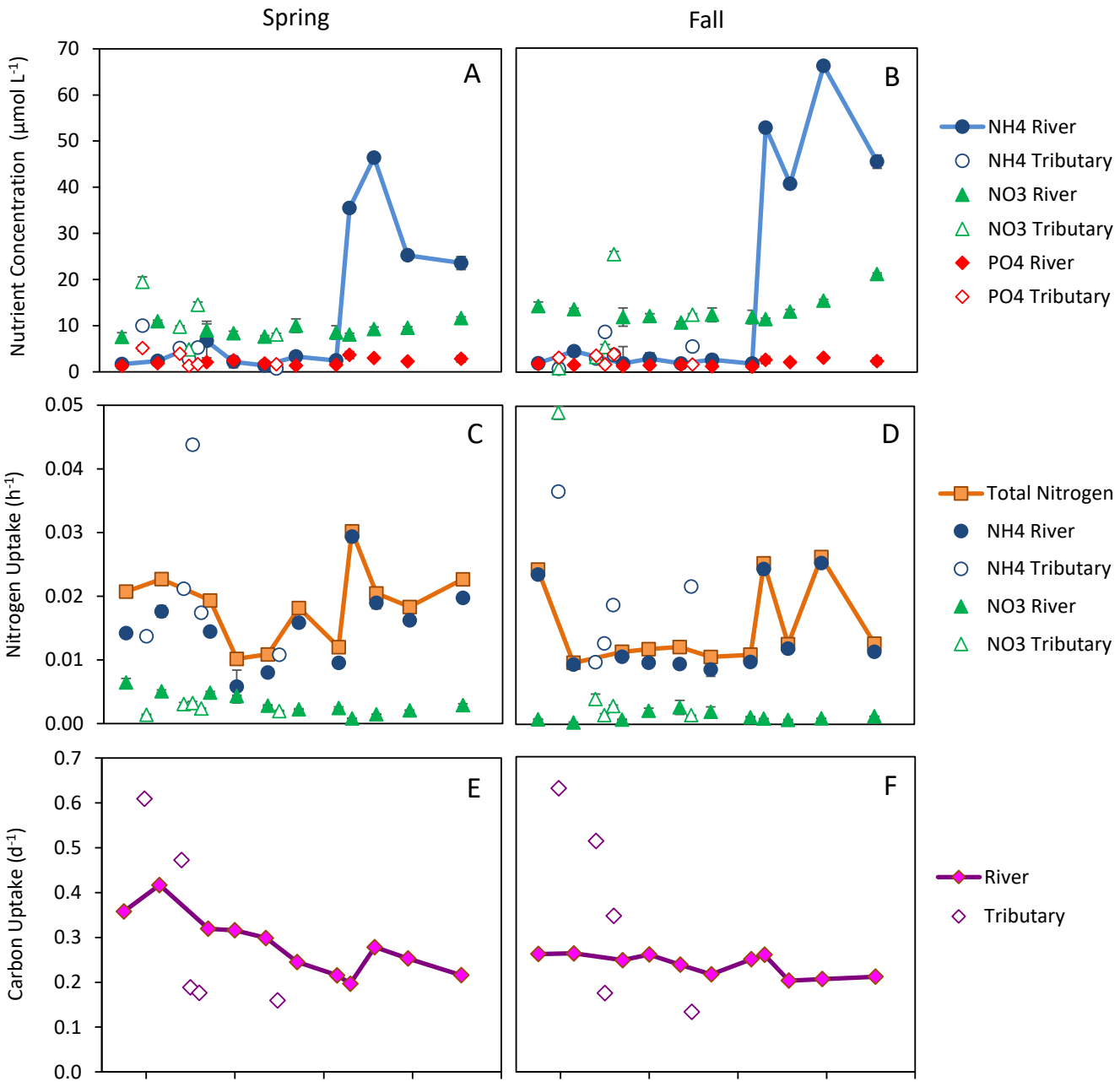

Figure 4 Concentrations (µmol L^{-1}) of NH_4^+ (*blue circles*), NO_3^- (*green triangles*), and PO_4^{3-} (*red diamonds*) along the lower Sacramento River mainstem (*solid*) and its tributaries (*open*) in (**A**) spring and (**B**) fall seasons. Contribution of total nitrogen uptake (h^{-1}) comprised NH_4^+ uptake (*blue circles*) and NO_3^- uptake (*green triangles*) along the lower Sacramento River mainstem (*solid*) and its tributaries (*open*) in (**C**) spring and (**D**) fall seasons. Mean ± standard error, with 3 replicates per station. Phytoplankton growth rates estimated from carbon uptake measurements (d^{-1}) as a function of river mile in the lower Sacramento River (*solid*) and in its tributaries (*open*) in the (**E**) spring and (**F**) fall seasons. Mean ± standard error, with 6 replicates per station.

with the average (0.023 h^{-1}) for the four stations downstream of the outfall (RM 44 to RM 19); t(6) = -3.2, p = 0.019. During the fall, NH_4^+ contributed 88% of the total nitrogen uptake above SRWTP's outfall and 94% below (Figure 4D). In the fall, the average total nitrogen uptake rate from RM 70 to RM 47 (0.011 h^{-1}) was similar to the average total nitrogen uptake rate from RM 44 to RM 19 (0.019 h^{-1}); t(6) = –2.05, p = 0.086. The greatest total nitrogen uptake in the fall occurred in the Colusa Basin Drain (0.037 h^{-1}), where NH_4^+ contributed 43% and NO_3^- contributed 57% of total nitrogen uptake. The concentrations of nitrogen remaining in the incubation bottles at the end of the uptake incubation period—which varied from 7 to 20 µmol L^{-1} during both the spring and fall surveys—indicated that nitrogen concentrations were likely not limiting phytoplankton biomass accumulation at any of the sampled locations.

Phytoplankton growth rates (d^{-1}), estimated from carbon uptake rates (h^{-1}), declined from 0.42 d^{-1} to 0.20 d^{-1} between RM 87 and RM 44 in the mainstem during spring (Figure 4E). The highest growth rates, 0.61 d^{-1} and 0.47 d^{-1}, occurred in the Colusa Basin Drain and East Canal, respectively. During fall, phytoplankton growth rates remained high in the Colusa Basin Drain and East Canal, at 0.63 d^{-1} and 0.51 d^{-1}, respectively, but rates decreased markedly in the mainstem, from 0.26 d^{-1} to 0.20 d^{-1} (Figure 4F). During both seasons, mean phytoplankton growth rates at the four sample locations downstream of the SRWTP outfall were not significantly different from those occurring at the four sample locations immediately upstream of the outfall; t(6) = 1.29, p = 0.244 (spring, Figure 4E), t(6) = 1.11, p = 0.310 (fall, Figure 4F).

Chlorophyll-a Concentrations and Phytoplankton Community Composition

In the spring, Chl-*a* concentrations decreased from a high of 14 µg L^{-1} at RM 95 to a low of 1.8 µg L^{-1} at RM 19 (Figure 5A). Chl-*a* concentrations in the Colusa Basin Drain, East Canal, and Natomas Cross Canal varied from 13.3 to 18.5 µg L^{-1} but were much lower in the Feather and American rivers, varying from 1.5 to 2.0 µg L^{-1}. In fall, Chl-*a* concentrations were substantially lower along the mainstem than in spring, and declined from 4.0 µg L^{-1} at RM 87 to 2.0 µg L^{-1} at RM 19 (Figure 5B). However, Chl-*a* concentrations remained high in the Colusa Basin Drain, East Canal, and Natomas Cross Canal in the fall, varying from 10.0 to 55.3 µg L^{-1}.

Diatoms (Bacillariophyta) dominated phytoplankton community composition (80% to 98%), based on cell volumes, along all Sacramento River mainstem stations in both spring and fall (Figure 6A and 6B). In both seasons, the genera *Melosira*, *Synedra* and *Diatoma* were dominant, with *Melosira* sp. dominating in spring and *Synedra ulna* dominating in fall (Appendix B, Supplemental Table 1). The non-diatom portion of the phytoplankton community along the mainstem was composed principally of cryptophytes (*Rhodomonas* sp.) and chlorophytes (*Chlorella* sp.) in spring, whereas in fall it was composed of multiple taxonomic groups including cryptophytes, chlorophytes, cyanobacteria, and picoplankton (Figure 6A and 6B; Appendix B, Supplemental Table 1). Many species of *Chlorella* are around 2 µm in diameter (e.g., Berg et al. 2017) and could be included in the picoplankton; here, *Chlorella* sp. were not included in the picoplankton enumerations. Picoplankton represented a small portion of the Sacramento River phytoplankton biomass, averaging 0.4 ± 0.1% (mean ± SE) of the community composition in spring and 1.8 ± 2% in fall. Phytoplankton taxa in the tributaries were either similar to those in the mainstem, as we observed in the Feather River and American River where diatoms were dominant, or were notably different, as we observed in the Colusa Basin Drain, East Canal, and Natomas Cross Canal, where cryptophytes and chlorophytes composed large proportions of the communities (Figure 6A and 6B; Appendix B, Supplemental Table 1).

Zooplankton Abundance and Grazing

Zooplankton biomass showed a strong seasonality, with 14-fold higher biomass in spring than fall (Figure 5C and 5D). In spring, average zooplankton biomass was much greater in the Colusa Basin Drain and East Canal (27 ± 3 µg dw L^{-1} [mean ± SE] and 41 ± 6 µg dw L^{-1},

https://doi.org/10.15447/sfews.2023v21iss1art3

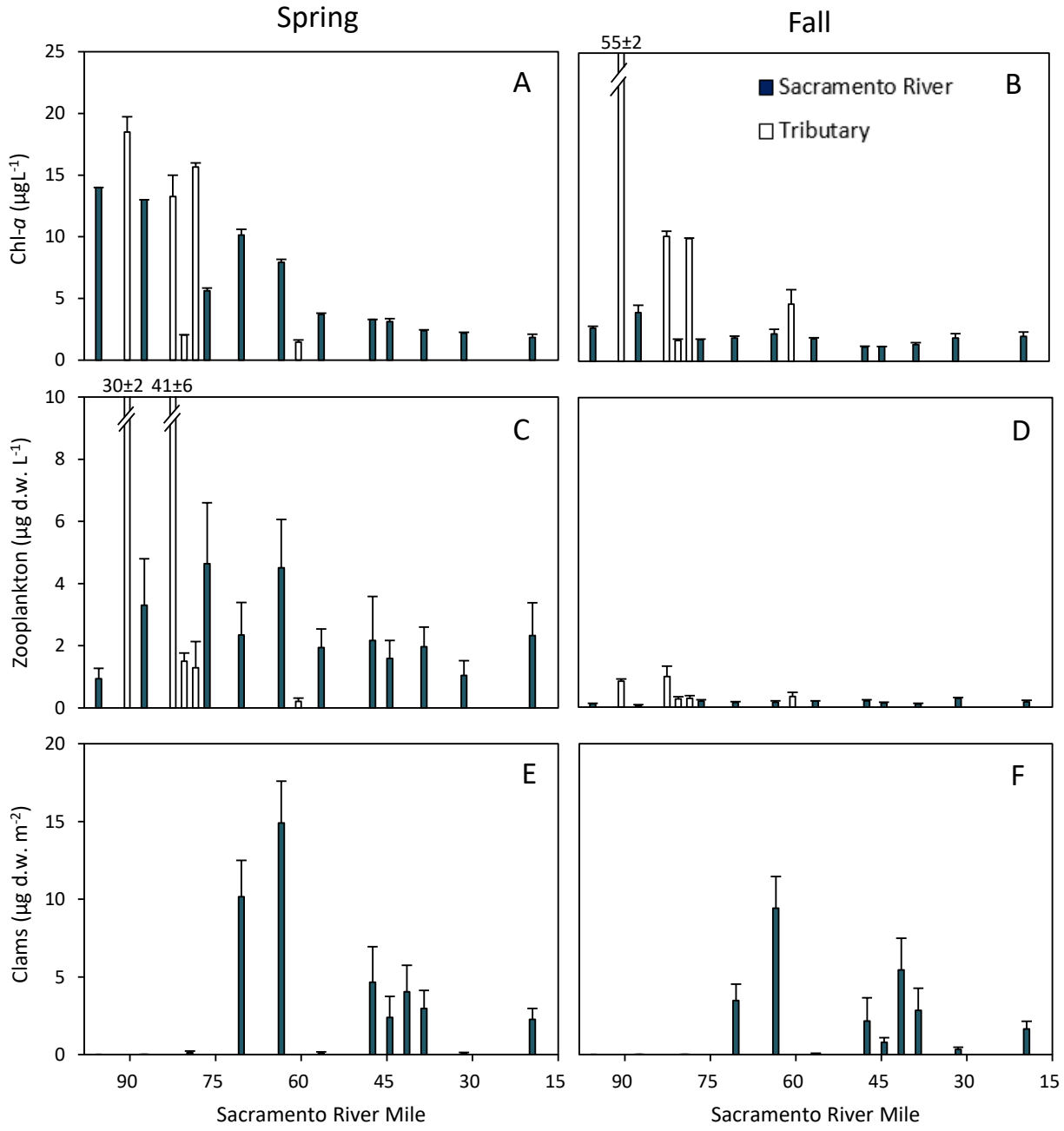

Figure 5 Concentrations of Chl-*a* (µg L^{-1}, n = 3) as a function of river mile in lower Sacramento River (*dark bars*) and its tributaries (*white bars*) in the (**A**) spring and (**B**) fall seasons. Mean biomass of zooplankton (µg dw L^{-1}, n = 3) as a function of river mile in the (**C**) spring and (**D**) fall seasons. Biomass of clams (g m^{-2}, n = 5) as a function of river mile in the (**E**) spring and (**F**) fall seasons. Mean ± standard error, with *n* replicates per station.

respectively) than in the Sacramento River mainstem, where average biomass ranged from 1 to 5 µg dw L^{-1}. Zooplankton biomass was also elevated in the Colusa Basin Drain and East Canal during the fall compared to the Sacramento River mainstem, but the differences among these tributaries and the mainstem (up to 5-fold) were less than those observed in spring. Zooplankton biomass in the Feather River, Natomas Cross Canal, and American River was low in both seasons. Cladocerans contributed the most to macrozooplankton biomass, with cyclopoid

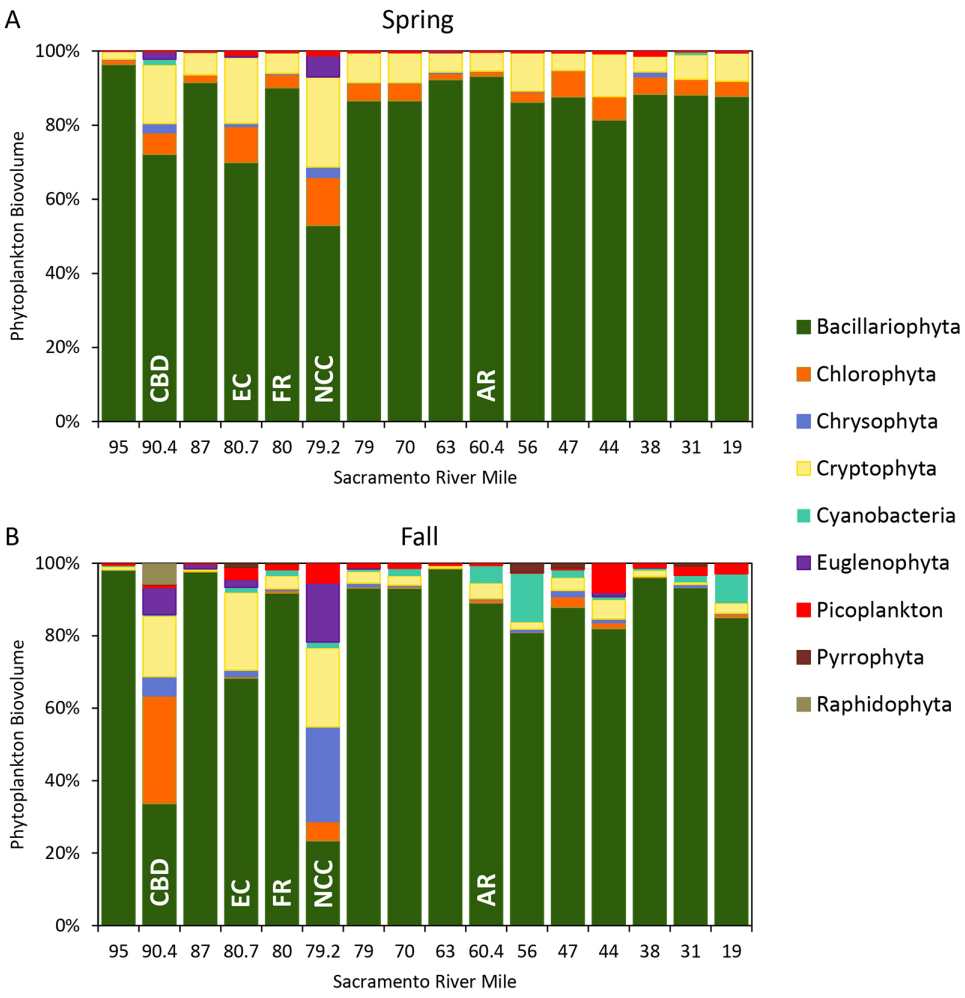

Figure 6 Average phytoplankton community composition by major division based on biomass ($\mu m^3 L^{-1}$) expressed as a percent of total biovolume in the lower Sacramento River and in its tributaries in (A) spring and (B) fall, with 3 replicates per station. CBD = Colusa Basin Drain; EC = East Canal; FR = Feather River; NCC = Natomas Cross Canal; AR = American River.

copepods co-dominant in the Sacramento River mainstem, particularly the genus *Acanthocyclops*. Zooplankton grazing rates computed for the mainstem, based on mean zooplankton biomass, varied from 0.0003 d^{-1} to 0.006 d^{-1} in spring and from 0.0002 d^{-1} to 0.0009 d^{-1} in fall (Table 2).

Clam Abundance and Grazing

C. fluminea was the only bivalve species found in our benthic clam trawls. Clam biomass was highest at RM 70 and RM 63 in both the spring and fall (Figure 5E and 5F) and was almost absent upstream of RM 70. *C. fluminea* occurred in low to moderate abundance from RM 56 to RM 19. *C. fluminea* filtering rates reached as high as 1.7 $m^3 m^{-2} d^{-1}$ in spring and 0.6 $m^3 m^{-2} d^{-1}$ in fall, between RM 70 and RM 63, resulting in water column turnover rates by clams of 0.54 d^{-1} and 0.23 d^{-1} in the spring and fall, respectively (Table 2).

Chlorophyll-*a* Mass Balance Calculations

We used mass balance calculations to assess the relative importance of dilution by tributary inflows, grazing losses, and light limitation to the declines in Chl-*a* observed in the Sacramento River mainstem in the spring and fall. The concentration of NH_4^+ was not included as a loss factor in the mass balance calculation because carbon uptake and total nitrogen uptake increased in tandem with NH_4^+ concentrations (Figure 4), suggesting that NH_4^+ concentrations had a positive rather than a negative effect on phytoplankton growth and biomass accumulation.

https://doi.org/10.15447/sfews.2023v21iss1art3

Table 2 Phytoplankton growth rates, zooplankton grazing rates, and clam grazing rates along the lower portion of the Sacramento River. Appendix A contains growth and grazing-rate calculation methods.

	Phytoplankton	Zooplankton Grazing		Clam Grazing		
River Mile	Growth rate (d^{-1})	Chl-a consumed (μg Chl-*a* L^{-1} d^{-1})	Grazing rate (d^{-1})	Chl-a consumed (mg Chl-*a* m^{-2} d^{-1})	Filtration rate (m d^{-1})	Turnover rate (d^{-1})
Spring						
95	0.36	4.31E-03	3.08E-04	6.69E-03	0.00	1.04E-04
87	0.42	1.51E-02	1.16E-03	1.76E-02	0.00	2.82E-04
79	0.32	2.13E-02	2.22E-03	1.28E-01	0.01	4.93E-03
70	0.32	1.07E-02	1.06E-03	1.17E+01	1.16	5.03E-01
63	0.30	2.07E-02	2.61E-03	1.37E+01	1.73	5.40E-01
56	0.25	8.90E- 03	2.40E-03	3.25E-02	0.01	9.75E-04
47	0.22	9.94E-03	3.01E-03	1.60E+00	0.49	6.94E-02
44	0.20	7.28E-03	2.35E-03	7.28E-01	0.23	2.63E-02
39	0.28	9.02E-03	3.76E-03	6.17E-01	0.26	3.28E-02
31	0.25	4.78E-03	2.17E-03	1.95E-02	0.01	9.64E-04
19	0.22	1.07E-02	5.92E-03	3.56E-01	0.20	4.30E-02
Fall						
95	0.26	4.80E-04	1.78E-04	7.28E-04	0.00	7.52E-05
87	0.26	2.38E-04	6.00E-05	4.64E-03	0.00	2.78E-04
79	0.25	8.91E-04	5.04E-04	1.11E-03	0.00	2.62E-04
70	0.26	7.13E-04	3.76E-04	4.07E-01	0.21	9.26E-02
63	0.24	7.22E-04	3.23E-04	1.29E+00	0.58	2.30E-01
56	0.22	8.87E-04	4.84E-04	7.14E-03	0.00	4.55E-04
47	0.25	9.35E-04	8.01E-04	1.59E-01	0.14	1.71E-02
44	0.26	6.20E-04	5.17E-04	6.21E-02	0.05	7.37E-03
39	0.20	4.63E-04	3.39E-04	2.48E-01	0.18	2.28E-02
31	0.21	1.30E-03	6.85E-04	4.20E-02	0.02	2.26E-03
19	0.21	7.96E-04	3.92E-04	2.18E-01	0.11	2.83E-02

The total decline in Chl-*a* along the Sacramento River mainstem (RM 95 to RM 19) in spring was 12.2 $\mu g L^{-1}$ according to our measurements, compared with 8.7 $\mu g L^{-1}$ according to the mass balance calculation (Figure 7A). In fall, it was 0.7 $\mu g L^{-1}$ versus 0.2 $\mu g L^{-1}$ according to our measurements and calculation, respectively (Figure 7C). While the mass balance analysis reasonably reflected the reduction in Chl-*a* concentrations during the spring in the upper segment of the Sacramento River (RM 95 to RM 63), by the bottom of the lower river segment the predicted Chl-*a* concentration was three times greater than that observed. In other words, the mass balance calculation failed to explain 4.6 $\mu g L^{-1}$ (56%) of the measured decline in Chl-*a* between RM 63 and RM 19 during the spring (Figure 7A).

DISCUSSION

A combination of environmental factors contributed to the phytoplankton biomass decline along the Sacramento River between RM 95 and RM 19 (Figure 7B and 7D). These factors varied in magnitude between the upper reach (RM 95 to RM 63) and the lower reach (RM 63 to RM 19), as well as between seasons (Figure 8). Because differences in Chl-*a* were small in fall (< 1 $\mu g L^{-1}$ change in Chl-*a*), the following discussion emphasizes the spring season for the factors that drive the decline in Chl-*a*.

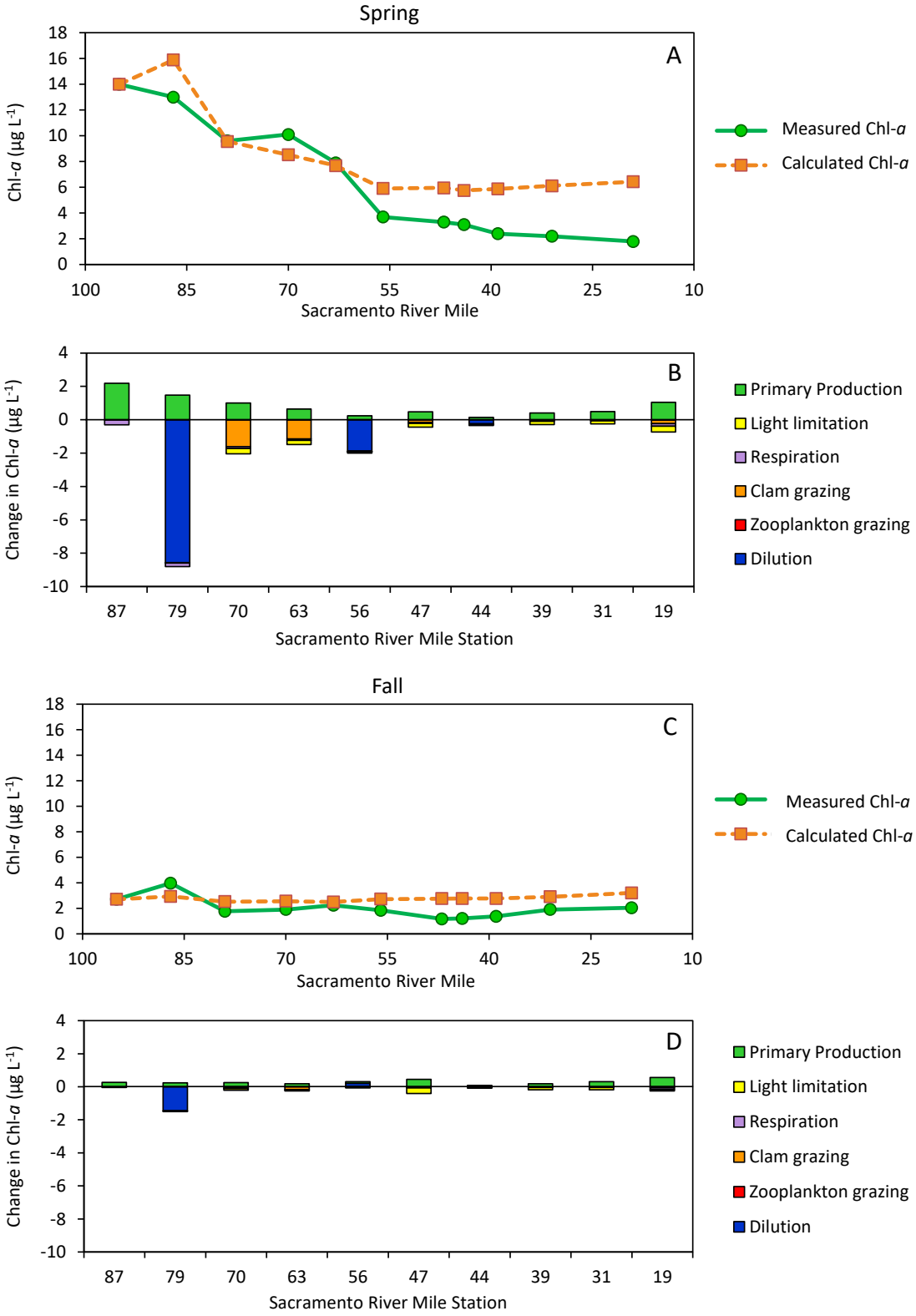

Figure 7 Comparison of average Chl-*a* concentrations from measured samples (n = 3) with Chl-*a* calculated using the mass balance described in Appendix A (**A**, **C**) and comparison of individual factors contributing to the calculated gains and losses in Chl-*a* between sampling stations in the lower Sacramento River (**B**, **D**) during spring (**A**, **B**) and fall (**C**, **D**).

https://doi.org/10.15447/sfews.2023v21iss1art3

Drivers of Chl-*a* Decline in the Upper Reach (RM 95 to RM 63)

We found that declines in Chl-*a* along the Sacramento River originated further upstream and occurred over a longer stretch than previously reported (e.g., Parker et al. 2012; Kraus et al. 2017). In the upper reach, the measured Chl-*a* concentration declined by roughly 50% from 14.0 to 7.7 $\mu g\,L^{-1}$ (Figures 5A, 7A, and 8). While the Feather River contributed 46% of the total volume of the Sacramento River below its confluence, it carried only 2 $\mu g\,L^{-1}$ Chl-*a*, serving to dilute the Sacramento River (Figures 2A and 5A). According to the mass balance calculation, dilution by the Feather River contributed 69% of the Chl-*a* decline in the spring (Figure 7B). It also had a comparable effect in the fall when the Feather River composed 40% of the downstream river flow while contributing only 1.7 $\mu g\,L^{-1}$ Chl-*a* (Figures 2B, 5B, and 7D).

Similar to the Feather River, the smaller tributaries influenced by agricultural run-off above RM 63—including the Colusa Basin Drain, East Canal, and the Natomas Cross Canal—did not contribute noticeable phytoplankton biomass to the Sacramento River mainstem. Although these tributaries had 1.4 to 2.0 times greater rates of phytoplankton growth and 1.4 to 16.4 times higher concentrations of Chl-*a*, their dominant phytoplankton genera—which included cryptophytes, chlorophytes, chrysophytes, and euglenophytes—were not evident in the mainstem. One reason for this could be that the agricultural tributaries lacked sufficient discharge to increase Sacramento River Chl-*a* concentrations. It is also possible that the conditions in the agricultural tributaries were so different in terms of hydrology and water quality that when transported from the tributary to the mainstem the phytoplankton ceased to grow.

The second driver of the Chl-*a* decline in the upper reach was grazing by clams and macrozooplankton, contributing 25% (Figures 7B and 8). In comparison to grazing by clams, grazing by zooplankton was negligible (Figure 7B). Adult zooplankton grazing rates estimated here, varying from 0.0003 d^{-1} to 0.006 d^{-1} in spring, were comparable to the lower end of grazing rates measured for adult *Pseudodiaptomus*, and an order of magnitude lower than grazing rates measured for adult *Eurytemora* in the low-salinity zone of the Delta (Kimmerer et al. 2014). We estimate that zooplankton grazing explained only 0.2% of the total Chl-*a* decline observed during the spring in the upper reach and 0.01% in the lower reach. This is consistent with other modeling approaches specific to the estuary and Delta systems, which found grazing by macrozooplankton to be less important than grazing by clams (Cloern 1982; Lucas et al. 1999; Lopez et al. 2006).

The effect of clam grazing on phytoplankton biomass is greatest in a shallow, fully mixed water body, because clams can filter the entire water column more rapidly relative to a deeper water body (Lucas and Thompson 2012). However, in a system with minimal sediment re-suspension, the effect of grazing can be compensated for by an increase in phytoplankton productivity and growth rate if the clearing of phytoplankton increases light availability and nutrient concentrations (Caraco et al. 1997). In a turbid system like the Sacramento River with constant sediment re-suspension, loss of phytoplankton biomass is not compensated for by increased productivity in the remaining phytoplankton.

In the present study, *C. fluminea* biomass was highest above the confluence with the American River, between RM 70 to RM 63 in both the spring and fall, suggesting that this 11-km stretch of river was conducive to the establishment and persistence of *C. fluminea*. In this region, where water depths were shallow and phytoplankton biomass was relatively high, clams could filter roughly 50% of the water column per day in the spring (Table 2). However, phytoplankton traveled through this region relatively quickly, in about 13 h, minimizing their contact time with grazers among the benthos. The average percentage of the water column turned over by *C. fluminea* grazing (turnover rate) at 11 stations located across the Delta and Suisun Bay ranged from 0.02 to 0.62 d^{-1}, as monitored monthly by the benthic monitoring program element of the

Environmental Monitoring Program (EMP) from 1996 to 2013 (Crauder et al. 2016). The average clam turnover rate in the Sacramento River during our study (0.07 d^{-1} across both seasons) was below the average turnover rate occurring at the closest EMP station (Rio Vista, 0.25 d^{-1}), but similar to other locations in the Delta (Sherman Lake 0.08 d^{-1} and the Sacramento River near Sherman Island 0.02 d^{-1}). Because of slow phytoplankton growth rates in the Delta, clam turnover rates that exceed 0.20 d^{-1} are expected to limit phytoplankton growth (Crauder et al. 2016). Although the overall grazing effect of *C. fluminea* on phytoplankton biomass along our study region of the Sacramento River was generally small, clam turnover rates in the spring at Sacramento RM 70 (0.50 d^{-1}) and RM 63 (0.54 d^{-1}) resulted in a notable phytoplankton decline according to our mass balance calculation. In regions outside RM 70 to RM 63, reduced effects from clam grazing could potentially be a result of reduced filtration efficiencies that result from relatively high water velocities (Cole et al. 1992; Ackerman 1999).

In comparison to dilution by the Feather River and grazing by clams, light limitation played a small role in the Chl-*a* decline, on the order of 5% of the total reduction in the upper reach (Figures 7B and 8). In this region, where station depth on average was 3.3 m, the euphotic zone nearly reached the bottom of the river (Figure 3), potentially allowing phytoplankton to grow without being limited by light throughout the water column.

Drivers of Chl-*a* Decline in the Lower Reach (RM 63 to RM 19)

Similar to the upper reach, the dominant driver of the decline in Chl-*a* in the lower reach during the spring was dilution, this time by the American River, contributing approximately 26% of the decline according to the mass balance calculation (Figures 7B and 8). Because of the lower abundance of clams in the lower reach (Figure 5E), Chl-*a* losses from grazing were over 4-fold less compared with the upper reach, contributing 6% of the total loss according to the mass balance calculation (Figures 7B and 8).

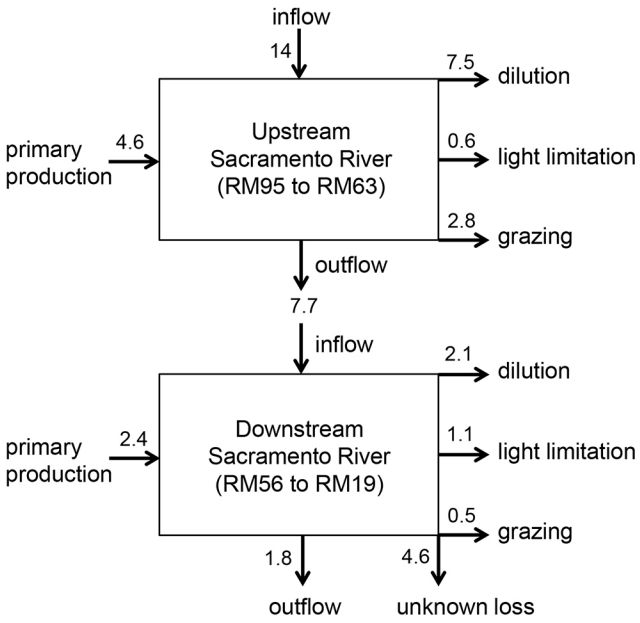

Figure 8 Spring Chl-*a* mass balance (µg L^{-1}) for RM 95 to RM 63 (*upper box*) and RM 63 to RM 19 (*lower box*) according to calculations described in Appendix A and in the text. Inflow is set to the Chl-*a* concentration measured at RM 95 in spring. Unknown Chl-*a* loss factor is the difference between outflow from the *bottom box* calculated via the mass balance and the Chl-*a* concentration measured at RM 19.

https://doi.org/10.15447/sfews.2023v21iss1art3

In contrast to the upper region, the increase in depth between RM 56 and RM 31 meant that phytoplankton spent less time in the euphotic zone and more time below the euphotic zone where there was not enough light to support photosynthesis and growth. As a result, phytoplankton growth rates (i.e., the input to our mass balance calculation) decreased, with light limitation contributing 13% to the decline in Chl-*a* in this reach. For a range of estuaries and rivers, Cloern (1987) found that phytoplankton productivity declines to zero when the ratio of the euphotic zone depth to mixed depth (Z_{eu}:Z_m) is 0.2 or less. This is because when phytoplankton spend only 20% of their time exposed to sufficient light for photosynthesis, respiratory carbon losses equal gains by photosynthesis and net growth is zero. The closer the Z_{eu}:Z_m ratio is to 0.2, the slower phytoplankton growth will be. Here, the Z_{eu}:Z_m ratio varied from 0.2 to 0.5 in the region between RM 63 and RM 31, depending on station location and season, suggesting that growth of phytoplankton in this region was restricted by light availability to a greater degree than in the upper reach where the ratio varied from 0.5 to 1.0.

Other Factors Potentially Contributing to Phytoplankton Decline in the Lower Reach

Although we estimated Chl-*a* declines from dilution, light limitation, and grazing in our mass balance calculation, close to 56% of the measured decline of Chl-*a* in the lower river reach was unaccounted for during the spring (Figure 8). Because the most abrupt declines in Chl-*a* in the Sacramento River occurred immediately below the confluence of the American River, it is unclear whether the factors that resulted in this decline were associated with changes in the Sacramento River itself or in its blending with American River water. Other factors that were not the focus of our study might have contributed to phytoplankton biomass losses in the lower river segment, potentially including increased microzooplankton grazing (e.g., Kimmerer and Thompson 2014), toxicity from mixtures of pesticide and herbicide contaminants (Domagalski 2000; Orlando et al. 2014), settling of benthic diatoms, and physiological stress from changes in pH and alkalinity (e.g., MacDougall et al. 2017) resulting from mixing of American River water with Sacramento River water, to mention a few.

For example, Kimmerer and Thompson (2014) estimated that microzooplankton can graze up to 67% d^{-1} of phytoplankton growth in shallow water shoals in Suisun Bay. However, in their study microzooplankton grazed less than 3% d^{-1} of phytoplankton biomass in regions where water depths exceeded 5 m. The average water depth in the lower reach where the unexplained Chl-*a* decline occurred in the Sacramento River was 7.6 m. In a separate but related study, we investigated microzooplankton grazing rates using the dilution bioassay methods of Landry and Hassett (1982). Using this technique we found no noticeable evidence of microzooplankton grazing in Sacramento River water collected at RM 70 (Appendix B, Supplemental Figure 2). Therefore, we find it unlikely that grazing by microzooplankton could account for the unexplained Chl-*a* decline. We also measured concentrations of contaminants during the current study (data not shown) and did not find concentrations of dissolved pesticides or herbicides at levels known to limit phytoplankton—particularly diatom—growth or reproduction (e.g., Stout et al. 2018; Lam et al. 2019).

The hydrological conditions in the lower Sacramento River likely selected for the dominant diatom taxa we encountered (e.g., Wehr and Descy 1998). Our study supports the finding by Kraus et al. (2017) that the majority of phytoplankton biomass in the pelagic zone of the Sacramento River is composed of benthic diatoms (Appendix A, Supplemental Table 1). Benthic diatoms are also known to dominate phytoplankton biomass in many large rivers and estuaries worldwide, including Japan (Kasim and Mukai 2006), France (Tekwani et al. 2013), and China (Wang et al. 2019). Most benthic diatoms can grow slowly in the dim light at the river bottom and rapidly when they become suspended in the water column (Reynolds and Descy 1996; Reynolds 2006; Beaver et al. 2013). The benthic life stage for diatoms living in large river systems has been theorized to be an adaptation to avoid

population washout (Reynolds and Descy 1996; Istvànovic and Honti 2011).

The most obvious change in the Sacramento River at RM 63 is a large increase in water column depth, which greatly exceeds the euphotic zone and restricts light at the river bottom (Figure 3), coupled with a transition to a tidally influenced portion of the river. Under moderate outflows, the Sacramento River below RM 63 transitions from a unidirectional outflow to a pattern of regular flow reductions or reversals from tidal forcing. It is possible that the transition to a more tidally influenced portion of the Sacramento River could have increased diatom sinking and deposition during slack tides. Then, weaker reverse river flows generated by flood tides might be sufficient to mobilize river sediments but insufficient to re-suspend the settled diatoms, resulting in the deposited cells becoming buried in the sediments (Jenness and Duineveld 1985). Benthic diatoms settling out of the water column in this deep region of the river—as a result of tidal action and hydrological changes related to the confluence with the American River, coupled with lack of light—may experience substantial stress and eventual mortality. We did not account for settling of benthic diatoms and eventual mortality at the river bottom in our mass balance calculation.

As mentioned above, the Sacramento River's confluence with the American River is a region with large hydrological changes as a result of this merging of two rivers as well as the action of the semi-diurnal tide. In addition to these physical factors, there may be changes in the Sacramento River's water chemistry that result from mixing with water from the American River. Past studies have shown that the alkalinity of the Sacramento River can be as high as 72 mg L^{-1} while the alkalinity of the American River can be as low as 20 mg L^{-1} (Schemel 1984; Domagalski and Dileanis 2000). Mixing of Sacramento River water with American River water decreases the alkalinity and hardness of the Sacramento River (Schemel 1984). Whether this mixing of water with different chemistries plays a role in causing the stress to the phytoplankton community and the ensuing decline of Chl-*a* below the confluence of the American River is not known. However, recent investigations have demonstrated that diatoms in particular are sensitive to fluctuations in pH and alkalinity, and that such changes can lead to mass population mortalities (Potapova and Charles 2003; Smol and Stoermer 2010; MacDougall et al. 2017). Sudden declines in phytoplankton biomass (i.e., "crashing" of a bloom) may be induced by physiological stress followed by compromised integrity of the cells and subsequent loss in buoyancy (Visser et al. 1995; Tallberg and Heiskanen 1998; Berg et al. 2011). Consistent with the occurrence of broken diatom frustules and increased flocculation of organic material in our samples, diatoms collected in water grab samples from the Sacramento River by Kraus et al. (2017) also exhibited increased signs of decay at stations downstream of RM 60.

CONCLUSIONS

Phytoplankton decline in the lower Sacramento River was the result of a combination of physical and biological factors, which differed among regions and between seasons. In the upper reach, the largest contributors to declines in phytoplankton biomass were dilution by the Feather River and grazing by clams. In the lower reach, the largest contributors were an unknown loss factor, followed by dilution by the American River and slowed phytoplankton growth because of light limitation. It is important to note that our study occurred during a below-normal water year and only provided a snapshot of the range of conditions present in the Sacramento River. Other factors that regulate Chl-*a* concentrations might be dominant under different environmental conditions.

Future research to help evaluate the unexplained decline in Chl-*a* concentrations occurring below RM 63 in the Sacramento River could include conducting additional studies to evaluate microzooplankton grazing rates (Calbet et al. 2008), conducting comprehensive suspect screening analyses to identify the presence of currently undetected toxic chemicals (Moschet et al. 2017), surveying the biovolume and re-suspension rates of benthic diatoms at the

https://doi.org/10.15447/sfews.2023v21iss1art3

sediment surface (Newbold et al. 2005; Kasim and Mukai 2006), and investigating phytoplankton physiological stress and buoyancy in mixtures of American River and Sacramento River water. Some regions of the lower Sacramento River may simply be too deep and dark to support robust growth of the benthic diatom populations that compose the bulk of the phytoplankton biovolume in this system. Investigating the physical and biological conditions present in the Sacramento River above RM 95 might also reveal a different combination of environmental factors that can support seasonally robust benthic diatom growth (Chl-*a* > 10 µg L^{-1}). Increased understanding of the factors that influence Chl-*a* biomass throughout the Sacramento River will benefit restoration programs seeking to enhance pelagic food availability to support higher trophic-level organisms that inhabit Delta channels or other large river systems.

ACKNOWLEDGEMENTS

We thank John Beaver and BSA Environmental Services, Inc. for phytoplankton and zooplankton enumerations; Andy Hernandes and Anya Epstein for help with clam sample analyses; Srividhya Ramamoorthy, Gisela Cluster, and other members of the Regional San Environmental Laboratory for experimental design, sampling and analytical support; several reviewers who helped us improve the manuscript; and the Sacramento Regional County Sanitation District Board of Directors for approving funding for this project.

REFERENCES

Ackerman JD. 1999. Effect of velocity on the filter feeding of dreissenid mussels (*Dreissena polymorpha* and *Dreissena bugensis*): implications for trophic dynamics. Can J Fish Aquat Sci. [accessed 2020 Jun 29];56:1551–1561. *https://doi.org/10.1139/f99-079*

Alpine AE, Cloern JE. 1988. Phytoplankton growth rates in a light-limited environment, San Francisco Bay. Mar Ecol Prog Ser. [accessed 2020 Jun 29];44:167–173. *https://www.int-res.com/articles/meps/44/m044p167.pdf*

Beaver JR, Tietjen TE, Blasius–Wert BJ, Kirsch JE, Rosati TC, Holdren GC, Kennedy EM, Hollis RM, Teacher CE, Buccier km, et al. 2010. Persistence of *Daphnia* in the epilimnion of Lake Mead, Arizona–Nevada, during extreme drought and expansion of invasive quagga mussels (2000–2009). Lake Reserv Manag. [accessed 2020 Jun 29];26:273–282. *https://doi.org/10.1080/07438141.2010.519858*

Beaver JR, Jensen DE, Casamatta DA, Tausz CE, Scotese KC, Buccier km, Teacher CE, Rosati TC, Minerovic AD, Renicker TR. 2013. Response of phytoplankton and zooplankton communities in six reservoirs of the middle Missouri River (USA) to drought conditions and a major flood event. Hydrobiologia. [accessed 2020 Jun 29];705:173–189. *https://doi.org/10.1007/s10750-012-1397-1*

Beck MW, Jabusch TW, Trowbridge PR, Senn DB. 2018. Four decades of water quality change in the upper San Francisco Estuary. Estuar Coast Shelf Sci. [accessed 2020 Jun 29];212:11–22. *https://doi.org/10.1016/j.ecss.2018.06.021*

Berg GM, Mills MM, Long CM, Bellerby R, Strass V, Savoye N, Röttgers R, Croot PL, Webb A, Arrigo KR. 2011. Variation in particulate C and N isotope composition following iron fertilization in two successive phytoplankton communities in the Southern Ocean. Global Biogeochem Cy. [accessed 2022 May 5];25:535–554. *https://doi.org/10.1029/2010GB003824*

Berg GM, Driscoll S, Hayashi K, Ross M, Kudela R. 2017. Variation in growth rate, carbon assimilation, and photosynthetic efficiency in response to nitrogen source and concentration in phytoplankton isolated from upper San Francisco Bay. J Phycol. [accessed 2022 Apr 22];53(3):664–679. *https://doi.org/10.1111/jpy.12535*

Boynton WR, Kemp WM, Keefe CW. 1982. A comparative analysis of nutrients and other factors influencing estuarine phytoplankton production. In: Kennedy VS, editor. Estuarine comparisons. Proceedings of the Sixth Biennial International Estuarine Research Conferenc;, Gleneden Beach, OR, 1981 November 1–6. New York (NY): Academic Press. [accessed 2020 Jun 29]; p. 69–90. *https://doi.org/10.1016/B978-0-12-404070-0.50011-9*

Brown LR, Kimmerer W, Conrad JL, Lesmeister S, Mueller–Solger A. 2016. Food webs of the Delta, Suisun Bay, and Suisun Marsh: an update on current understanding and possibilities for management. San Franc Estuary Watershed Sci. [accessed 2020 Jun 29];14(3). *https://doi.org/10.15447/sfews.2016v14iss3art4*

Calbet A, Trepat I, Almeda R, Saló V, Saiz E, Movilla JI, Alcaraz M, Yebra L, Simó R. 2008. Impact of micro- and nanograzers on phytoplankton assessed by standard and size-fractionated dilution grazing experiments. Aquat Microb Ecol. [accessed 2020 Nov 13];50(2):145–156. *https://doi.org/10.3354/ame01171*

Caraco NF, Cole JJ, Raymond PA, Strayer DL, Pace ML, Findlay SEG, Fischer, DT. 1997. Zebra mussel invasion in a large, turbid river: phytoplankton response to increased grazing. Ecology. [accessed 2020 Jun 29];78:588–602. *https://doi.org/10.1890/0012-9658(1997)078[0588:ZMIIAL]2.0.CO;2*

[CDWR] California Department of Water Resources 2020. Dayflow results 1997–2019.csv [accessed 2020 Oct 30]. *https://data.cnra.ca.gov/dataset/dayflow*

Cloern JE. 1982. Does the benthos control phytoplankton biomass in south San Francisco Bay? Mar Ecol Prog Ser. [accessed 2020 Jun 29];9:191–202. *https://www.int-res.com/articles/meps/9/m009p191.pdf*

Cloern JE. 1987. Turbidity as a control on phytoplankton biomass and productivity in estuaries. Continental Shelf Research, [accessed 2022 Apr 14];7(11–12):1367–1381. *https://doi.org/10.1016/0278-4343(87)90042-2*

Cloern JE, Jassby AD. 2012. Drivers of change in estuarine-coastal ecosystems: discoveries from four decades of study in San Francisco Bay. Rev Geophys. [accessed 2020 Jun 29];50:133. *https://doi.org/10.1029/2012RG000397*

Cloern JE, Foster S, Kleckner A. 2014. Phytoplankton primary production in the world's estuarine–coastal ecosystems. Biogeosciences. [accessed 2020 Jun 29];11:2477–2501. *https://doi.org/10.5194/bg-11-2477-2014*

Cloern JE. 2021. Use care when interpreting correlations: the ammonium example in the San Francisco Estuary. San Franc Estuary Watershed Sci. [accessed 2022 Mar 10];19(4). *https://doi.org/10.15447/sfews.2021v19iss4art1*

Cole BE, Cloern JE. 1984. Significance of biomass and light availability to phytoplankton productivity in San Francisco Bay. Mar Ecol Prog Ser. [accessed 2020 Jun 29];17:15–24. *http://www.int-res.com/articles/meps/17/m017p015.pdf*

Cole BE, Cloern JE. 1987. An empirical model for estimating phytoplankton productivity in estuaries. Mar Ecol Prog Ser. [accessed 2020 Jun 29];36:299–305. *https://www.int-res.com/articles/meps/36/m036p299.pdf*

Cole BE, Thompson JK, Cloern JE. 1992. Measurement of filtration rates by infaunal bivalves in a recirculating flume. Mar Biol. [accessed 2020 Jun 29];113:219–225. *https://doi.org/10.1007/BF00347274*

Crauder JS, Thompson JK, Parchaso F, Anduaga RI, Pearson SA, Gehrts K, Fuller H, Wells E. 2016. Bivalve effects on the food web supporting delta smelt—a long-term study of bivalve recruitment, biomass, and grazing rate patterns with varying freshwater outflow. [accessed 2020 Jun 29]. US Geological Survey Open-File Report 2016–1005. 216 p. *https://doi.org/10.3133/ofr20161005*

Dodds WK, Smith VH. 2016. Nitrogen, phosphorus, and eutrophication in streams. Inland Waters. [accessed 2022 Apr 8];6(2):155–164. *https://doi.org/10.5268/IW-6.2.909*

Domagalski JL. 2000. Pesticides in surface water measured at selected sites in the Sacramento River Basin, California, 1996–1998. US Geological Survey Water-Resources Investigations Report 00-4203. [accessed 2022 Apr 20]. 24 p. Available from: *https://pubs.usgs.gov/wri/2000/wri004203/pdf/wri004203.pdf*

Domagalski JL, Dileanis PD. 2000. Water-quality assessment of the Sacramento River Basin, California–water quality of fixed sites, 1996–1998. US Geological Survey National Water-Quality Assessment Program. Water-Resources Investigations Report 00-4247. [accessed 2020 Jun 30]. 44 p. Available from: *https://ca.water.usgs.gov/user_projects/sac_nawqa/Publications/WRIR_2000-4247/wrir004247.pdf*

Domagalski JL, Knifong DL, Dileanis PD, Brown LR, May JT, Connor V, Alpers C. 2000. Water quality in the Sacramento River Basin, California, 1994–98. US Geological Survey. Circular 1215. [accessed 2022 Apr 20]. Available from: *https://pubs.usgs.gov/circ/2000/circ1215/pdf/circ1215.pdf*

Dugdale RC, Wilkerson FP, Hogue VE, Marchi A, 2007. The role of ammonium and nitrate in spring bloom development in San Francisco Bay. Estuar Coast Shelf Sci. [accessed 2022 Jul 22];73:17–29. *https://doi.org/10.1016/j.ecss.2006.12.008*

Glibert PM, Capone DC. 1993. Mineralization and assimilation in aquatic, sediment, and wetland systems. In: Knowles R, Blackburn TH, editors. Nitrogen isotope techniques. New York: Academic Press. [accessed 2020 Jun 30]; p. 243–272. *https://doi.org/10.1016/B978-0-08-092407-6.50014-6*

Glibert PM, Dugdale RC, Wilkerson F, Alexander J, Antell E, Blaser S, Johnson A, Lee J, Lee T, Murasko S, et al. 2014. Major – but rare – spring blooms in 2014 in San Francisco Bay Delta, California, a result of the long-term drought, increased residence time, and altered nutrient loads and forms. [accessed 2022 Apr 20]; J Exp Mar Bio Ecol 460:8–18. *https://doi.org/10.1016/j.jembe.2014.06.001*.

Guerin M. 2018. Regional San project 3 documentation: hydraulic modeling to estimate proportional water sources to the lower Sacramento River. [accessed 2020 Jun 30]. Davis (CA) Resource Management Associates Technical Memorandum. 79 p. Available from: *https://www.regionalsan.com/post/sacramento-river-phytoplankton-studies-2016 rma_-_proportional_water_sources.pdf*

Hammock BG, Moose SP, Solis SS, Goharian E, Teh SJ. 2019. Hydrodynamic modeling coupled with long-term field data provide evidence for suppression of phytoplankton by invasive clams and freshwater exports in the San Francisco Estuary. Environ Manag. [accessed 2020 Jun 30];63:703–717. *https://doi.org/10.1007/s00267-019-01159-6*

Hillebrand H, Dürselen CD, Kivschtel D, Pollingsher M, Zohary T. 1999. Biovolume calculation for pelagic and benthic microalgae. J Phycol. [accessed 2020 Jun 30];35:403–424. *https://onlinelibrary.wiley.com/action/showCitFormats?doi=10.1046%2Fj.1529-8817.1999.3520403.x*

[IEP] Interagency Ecological Program, Martinez M, Rinde J, Flynn TM, Lesmeister S. 2020. 2020. Discrete water quality monitoring in the Sacramento–San Joaquin Bay–Delta, collected by the Environmental Monitoring Program, 1975–2019. ver 3. Environmental Data Initiative. [accessed 2020 Oct 29]. *https://doi.org/10.6073/pasta/dc1fd386c098c6b71132150eee7ee86c*

Istvànovic V, Honti M. 2011. Phytoplankton growth in three rivers: the role of meroplankton and the benthic retention hypothesis. Limnol Oceanogr. [accessed 2020 Jun 30];56(4):1439–1452. *https://doi.org/10.4319/lo.2011.56.4.1439*

Jassby AD, Cloern JE, Cole BE. 2002. Annual primary production: patterns and mechanisms of change in a nutrient-rich tidal estuary. Limnol Oceanogr. [accessed 2020 Jun 30];47(3):698–712. *https://doi.org/10.4319/lo.2002.47.3.0698*

Jassby AD. 2008. Phytoplankton in the upper San Francisco Estuary: recent biomass trends, their causes, and their trophic significance. San Franc Estuary Watershed Sci. [accessed 2020 Jun 30];6(1). *https://doi.org/10.15447/sfews.2008v6iss1art2*

Jenness MI, Duineveld GCA. 1985. Effects of tidal currents on chlorophyll a content of sandy sediments in the southern North Sea. Mar Ecol Prog Ser. [accessed 2022 Apr 15]21(3):283–287. *https://doi.org/10.3354/meps021283*

Kasim M, Mukai H. 2006. Contribution of benthic and epiphytic diatoms to clam and oyster production in the Akkeshi-ko estuary. J Oceanogr. [accessed 2020 Nov 13]62:267–281. *https://doi.org/10.1007/s10872-006-0051-9*

Kimmerer W. 2004. Open water processes of the San Francisco Estuary: from physical forcing to biological responses. San Franc Estuary Watershed Sci. [accessed 2020 Jun 30];2(1). https://doi.org/10.15447/sfews.2004v2iss1art1

Kimmerer WJ, Ignoffo TR, Slaughter AM, Gould AL. 2014. Food-limited reproduction and growth of three copepod species in the low-salinity zone of the San Francisco Estuary. J Plankton Res. [accessed 2020 Jun 30];36:722–735. https://doi.org/10.1093/plankt/fbt128

Kimmerer WJ, Thompson JK. 2014. Phytoplankton growth balanced by clam and zooplankton grazing and net transport into the low-salinity zone of the San Francisco Estuary. Estuaries Coasts. [accessed 2020 Jun 30];37:1202–1218. https://doi.org/10.1007/s12237-013-9753-6

Kimmerer WJ, Ignoffo TR, Kayfetz KR, Slaughter AM. 2018. Effects of freshwater flow and phytoplankton biomass on growth, reproduction, and spatial subsidies of the estuarine copepod *Pseudodiaptomus forbesi*. Hydrobiologia. [accessed 2020 Jun 30];807:113–130. https://doi.org/10.1007/s10750-017-3385-y

Kimmerer WJ, Gross ES, Slaughter AM, Durand JR. 2019. Spatial subsidies and mortality of an estuarine copepod revealed using a box model. Estuaries Coasts. [accessed 2020 Jun 30];42:218–236. https://doi.org/10.1007/s12237-018-0436-1

Kraus TEC, Carpenter KD, Bergmaschi BA, Parker AE, Stumpner EB, Downing BD, Travis NM, Wilkerson FP, Kendall D, Mussen TD. 2017. A river-scale Lagrangian experiment examining controls on phytoplankton dynamics in the presence and absence of treated wastewater effluent high in ammonium. Limnol Oceanogr. [accessed 2020 Jun 30];62:1234–1253. https://doi.org/10.1002/lno.10497

Lam CH, Kurobe T, Lehman PW, Berg M, Hammock BG, Stillway ME, Pandey PK, Teh SJ. 2019. Toxicity of herbicides to cyanobacteria and phytoplankton species of the San Francisco Estuary and Sacramento–San Joaquin River Delta, California, USA. J Environ Sci Health A Tox Hazard Subst Environ Eng. [accessed 2020 Jun 30];55(2):107–118. https://doi.org/10.1080/10934529.2019.1672458

Landry MR, Hassett RP. 1982. Estimating the grazing impact of marine micro-zooplankton. Mar Biol. [accessed 2020 Jun 30];67:283–288. https://doi.org/10.1007/BF00397668

Lehman PW, Mayr S, Mecum L, Enright C. 2010. The freshwater tidal wetland Liberty Island, CA was both a source and sink of inorganic and organic material to the San Francisco Estuary. Aquat Ecol. [accessed 2020 Nov 5];44:359–372. https://doi.org/10.1007/s10452-009-9295-y

Lopez CB, Cloern JE, Schraga TS, Little AJ, Lucas LV, Thompson JK, Burau JR. 2006. Ecological values of shallow-water habitats: implications for the restoration of disturbed ecosystems. Ecosystems. [accessed 2020 Jun 30];9:422–440. https://doi.org/10.1007/s10021-005-0113-7

Lucas LV, Koseff JR, Cloern JE, Monismith SG, Thompson JK. 1999. Processes governing phytoplankton blooms in estuaries. I: the local production-loss balance. Mar Ecol Prog Ser. [accessed 2020 Jun 30];187:1–15. https://doi.org/10.3354/meps187001

Lucas LV, Thompson JK. 2012. Changing restoration rules: exotic bivalves interact with residence time and depth to control phytoplankton productivity. Ecosphere. [accessed 2020 Oct 22];3:1–26. https://doi.org/10.1890/ES12-00251.1

McNabb CD. 1960. Enumeration of freshwater phytoplankton concentrated on the membrane filter. Limnol Oceanogr. [accessed 2020 Jun 30];5:57–61. https://doi.org/10.4319/lo.1960.5.1.0057

MacDougall MJ, Paterson AM, Winter JG, Jones FC, Knopf LA, Hall RI. 2017. Response of periphytic diatom communities to multiple stressors influencing lakes in the Muskoka River Watershed, Ontario, Canada. Freshw Sci. [accessed 2022 May 5];36:77–89. https://doi.org/10.1086/690144

Moschet C, Lew BM, Hasenbein S, Anumol T, Young, TM. 2017. LC- and GC-QTOF-MS as complementary tools for a comprehensive micropollutant analysis in aquatic systems. Environ Sci Technol. [accessed 2020 Nov 13];51:1553–1561. https://doi.org/10.1021/acs.est.6b05352

Müller–Solger A, Jassby A, Mueller–Navarra D. 2002. Nutritional quality of food resources for zooplankton (*Daphnia*) in a tidal freshwater system (Sacramento–San Joaquin River Delta). Limnol Oceanogr. [accessed 2020 Jul 1];47:1468–1467. *https://doi.org/10.4319/lo.2002.47.5.1468*

Newbold JD, Thomas SA, Minshall GW, Cushing CE, Georgian T. 2005. Deposition, benthic residence, and resuspension of fine organic particles in a mountain stream. Limnol Oceanogr. [accessed 2020 Nov 13];50:1571–1580. *https://doi.org/10.4319/lo.2005.50.5.1571*

Novick E, Senn DB. 2014. External nutrient loads to San Francisco Bay. Richmond (CA): San Francisco Estuary Institute. SFEI Technical Report Contribution Number 704. [accessed 2020 Jun 30]. 98 p. Available from: *https://www.sfei.org/documents/external-nutrient-loads-san-francisco-bay*

Orlando JL, McWayne M, Sanders C, Hladik M. 2014. Dissolved pesticide concentrations entering the Sacramento–San Joaquin Delta from the Sacramento and San Joaquin Rivers, California, 2012–2013. US Geological Survey Data Series 876. [accessed 2020 Jun 30]. 28 p. Available from: *http://doi.org/10.3133/ds876*

Parker AE, Dugdale RC, Wilkerson FP. 2012. Elevated ammonium concentrations from wastewater discharge depress primary productivity in the Sacramento River and the Northern San Francisco Estuary. Mar Pollut Bull. [accessed 2020 Jun 30];64(3):574–586. *https://doi.org/10.1016/j.marpolbul.2011.12.016*

Potapova M, Charles DF. 2003. Distribution of benthic diatoms in US rivers in relation to conductivity and ionic composition. Freshw Biol. [accessed 2022 May 5];48:1311–1328. *https://doi.org/10.1046/j.1365-2427.2003.01080.x*

Reynolds CS, Descy J-P. 1996. The production, biomass and structure of phytoplankton in large rivers. River Systems.[accessed 2020 Jun 30];10(1-4):161–187. *https://doi.org/10.1127/lr/10/1996/161*

Reynolds CS. 2006. Ecology of phytoplankton. [accessed 2023 Mar 21]. Cambridge (UK): Cambridge University Press. 535 p. Available from: *https://doi.org/10.1017/CBO9780511542145*

Schemel LE. 1984. Salinity, alkalinity, and dissolved and particulate organic carbon in the Sacramento River Water at Rio Vista, California, and at other locations in the Sacramento–San Joaquin Delta, 1980. US Geological Survey. Water-Resources Investigations Report 83-4059 [accessed 2022 May 5]. 45 p. *https://doi.org/10.3133/wri834059*

Smol JP, Stoermer EF. 2010. The diatoms: applications for the environmental and earth sciences. 2nd ed. Cambridge (UK): Cambridge University Press. 686 p.

Stout SM, Orlando JL, McWayne M, Sanders C, Hladik M. 2018. Dissolved pesticide concentrations in the lower Sacramento River and its source waters, California, 2016. US Geological Survey Open-File Report 2018–1153. [accessed 2020 Jun 30]. 24 p. *https://doi.org/10.3133/ofr20181153*

Strong AL, Mills MM, Huang IB, van Dijken GL, Driscoll SE, Berg GM, Kudela RM, Monismith SG, Francis CA, Arrigo KR. 2021. Response of lower Sacramento River phytoplankton to high-ammonium wastewater effluent. Elementa. [accessed 2022 Jul 22];9(1):040. *https://doi.org/10.1525/elementa.2021.040*

Tallberg P, Heiskanen AS. 1998. Species-specific phytoplankton sedimentation in relation to primary production along an inshore–offshore gradients in the Baltic Sea. J Plankton Res. [accessed 2022 May 5];20:2053–2070. *https://doi.org/10.1093/plankt/20.11.2053*

Tekwani N, Majdi N, Mialet B, Tornés E, Urrea–Clos G, Buffan–Dubau E, Sabater S, Tackx M. 2013. Contribution of epilithic diatoms to benthic–pelagic coupling in a temperate river. Aquat Microb Ecol. [accessed 2020 Nov 13];69:47–57. *https://doi.org/10.3354/ame01616*

Visser PM, Ibelings BW, Mur LR. 1995. Autumnal sedimentation of *Microcystis* spp. as result of an increase in carbohydrate ballast at reduced temperature. J Plankton Res. [accessed 2022 May 5];17:919–933. *https://doi.org/10.1093/plankt/17.5.919*

Wang J, Liu Q, Zhao X, Borthwick AGL, Liu Y, Chen Q, Ni J. 2019. Molecular biogeography of planktonic and benthic diatoms in the Yangtze River. Microbiome. [accessed 2020 Nov 13];7:153 *https://doi.org/10.1186/s40168-019-0771-x*

Wehr JD, Descy JP. 1998. Use of phytoplankton in large river management. J Phycol. [accessed 2020 Jul 24];34(5):741–749. *https://doi.org/10.1046/j.1529-8817.1998.340741.x*

https://doi.org/10.15447/sfews.2023v21iss1art3